MODELING OF WIND-WAVE GROWTH IN STRONG WIND CONDITIONS BASED ON PHASE-RESOLVING WAVE MODEL

Shoko Sato, Kyoto University, satou.shouko.35e@st.kyoto-u.ac.jp
Nobuhito Mori, Kyoto University, mori.nobuhito.8a@kyoto-u.ac.jp
Tomoya Shimura, Kyoto University, shimura.tomoya.2v@kyoto-u.ac.jp
Takuya Miyashita, Kyoto University, miyashita.takuya.4w@kyoto-u.ac.jp

INTRODUCTION

Recently, coastal disaste have occurred by typhoons passing through bays, such as Typhoon Jebi in 2018 and Typhoon Hagibis in 2019 (Mori et al.(2019), Shimozono et al.(2020)). Typhoon Jebi brought strong winds, storm surges, and high waves, causing extensive damage in Japan. The coastal area where Jebi passed was inundated, and Kansai International Airport was flooded because of the overtopping caused by high waves. These damages reduction demand the accurate evaluation of high wave deformation developing in a bay.

The current wave model cannot simultaneously account for the development of wind waves due to strong winds and wave deformation due to topography. In general, there are two wave models, one for the open ocean and the other for the inner bay. In the sea, a spectral wave model is used to simulate the development and propagation of wave energy (Pierson et al.(1955)). This model considers wave development caused by wind and breaking waves, but it cannot accurately evaluate wave deformation due to topography because it describes waves as energy. On the other hand, a phase-resolving wave model that solves the propagation of the wave shape is used in inner bays where the water level is less than 50 m (Hirayama, 2002). This wave model considers complex wave deformation due to topography, but wave development due to the wind is ignored. Therefore, the evaluation of waves developing in inner bays sits between these two models, and the way to deal with such waves is unclear.

This study aims to develop a phase-resolving wave model that considers the development of wind waves in shallow water under strong wind conditions. A wave development term that considers the local wave deformation is introduced into the phase-resolving wave model. XBeach (Roelvink et al., 2009) a numerical model based on the nonlinear long wave equation with non-hydrostatic pressure term, is used to calculate the waves in coastal areas. The wave development term is introduced, and the wave development process is optimized based on sensitivity experiments.

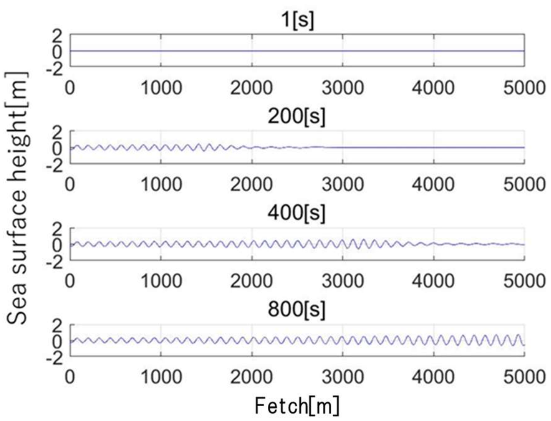

Figure 1 - Spatial distribution of wave (1, 200, 400, and 800 s after the first incident wave input) when regular waves are input under 30 m/s wind speed conditions

INTRODUCING A WAVE GROWTH TERM INTO A PHASE-RESOLVING WAVE MODEL

The wind stress term in the nonlinear long wave equation with non-hydrostatic pressure term is parameterized. A term based on Miles theory is added to the conventional stress term. The conventional wind stress term is

$$\frac{\rho_a}{\rho(\eta + h)} C_d \vec{U}|U|, \tag{1}$$

where ρ_a is the air density, ρ is the water density, η is the sea surface height, h is the water depth, and U is the wind speed at 10 m height. C_d is the momentum exchange coefficient (drag coefficient) in the bulk transport equation for momentum from wind to the sea surface. Using Honda-Mitsuyasu formula (Honda and Mitsuyasu, 1980), C_d is given by

$$C_d = (1.29 - 0.24U) \times 10^{-3}, U < 8\mathrm{m/s}, \tag{2a}$$

$$C_d = (0.581 + 0.063U) \times 10^{-3}, U \geq 8\mathrm{m/s}. \tag{2b}$$

An additional stress term based on Miles theory (Miles. 1957) is written in the form:

$$\frac{\rho_a}{\rho} \frac{2C_{miles}}{\kappa^2} \frac{\partial^2 \eta}{\partial x^2} C_d \vec{U}|U|. \tag{3}$$

Here, C_{miles} is the energy transport coefficient, κ is Karman constant that is 0.4. This term based on Miles theory is an expression that waves develop because of the local wave deformation.

The above wind stress term is introduced into XBeach, which is based on the nonlinear long wave equation considering non-hydrostatic pressure, to calculate wave deformation in coastal areas. For the sake of simplicity, the second-order derivative of η in Eq.(3) is discretized by approximating it as $k^2\eta$ where k is the wave number assuming quasi-monochromatic waves. Figure1 is a snapshot of sea surface height when regular waves with a wave height of 1 m and period of 10 s are input from the left boundary and develop on topography with a constant water depth of 20 m under uniform wind speed of 30 m/s. The value of C_{miles} is 0.06. The wave height increases as the fetch increases, indicating that the waves develop because of the introduced term.

PARAMETERIZATION OF THE WAVE DEVELOPMENT TERM

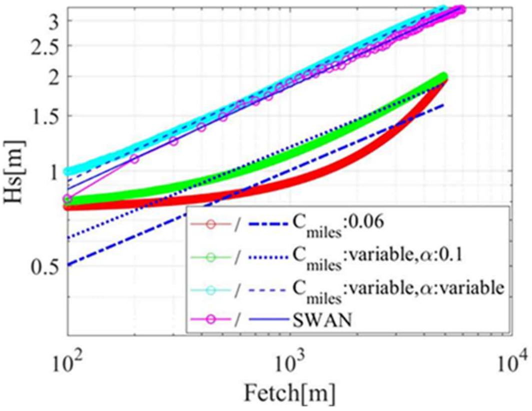

Figure 2 - Growth of significant wave height by proposed model and SWAN: U=30 m/s (red, blue dashed and dotted line: the result when C_{miles} is 0.06 and α is not introduced, green, blue dotted line: the result when C_{miles} is variable and α is 0.1, cyan, blue dashed line: the result when both C_{miles} and α are variable using Eq.(7) with the optimal value of $A = 0.9$, magenta, solid blue line: the result of SWAN)

The momentum flux from the wind to the sea surface is formulated as in Eq.(4a) and (4b). Although the momentum is formulated in the conventional wind stress term as being transported directly from wind to current, in fact the majority of the momentum is transported through wave dissipation (Mitsuyasu, 1985). The momentum τ from the wind to the sea surface is then formulated by dividing it into two parts: $\tau_{current}$ for the water surface drag force and $\tau_{develop}$ for the wave development.

$$\tau = \tau_{current} + \tau_{develop} = (1-\alpha)\rho_a u_*^2 + \alpha\rho_a u_*^2 \quad (4a)$$

$$\alpha = \frac{2\beta k^2 \overline{\eta^2}}{\kappa^2} \quad (4b)$$

Here, u_* is friction velocity, and β is the energy transport coefficient. For simplicity,

$$C_{miles} = \beta k^2. \quad (5)$$

Assuming that α is constant,

$$C_{miles} = \frac{\alpha\kappa^2}{2\overline{\eta^2}}. \quad (6)$$

C_{miles} is a function of the variance of the sea surface height $\overline{\eta^2}$. Therefore, as waves develop, C_{miles} becomes smaller and the momentum used for wave development becomes smaller.

To validate the assumption of dependence of wave energy on wave development, the spatial distribution of the significant wave heights are compared (Figure2). The result when $C_{miles} = 0.06$ and α is not introduced (red line) shows that the waves are overdeveloped, especially in the 100 m to 300 m and 4000 m to 5000 m fetch ranges. The green line shows the result when C_{miles} is a function of sea surface height and $\alpha = 0.1$ that means 90 % of the momentum is distributed to the current and 10 % to wave development. The result of this case shows that the excessive development of waves in those fetch ranges is smaller than in the case when fixed value of C_{miles} is used (red line). From these two results,

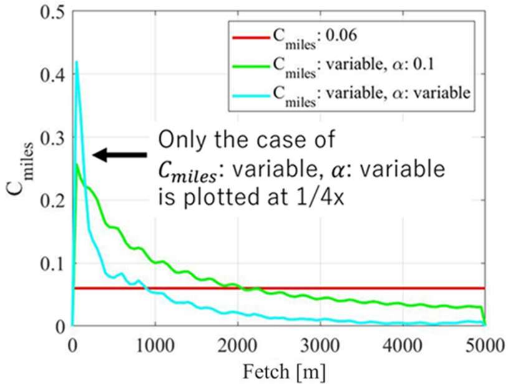

Figure 3 - Spatial distribution of C_{miles}: U=30 m/s, 3500 s after the first incident wave input (red: the result when C_{miles} is 0.06 and α is not introduced, green: the result when C_{miles} is variable and α is 0.1, cyan: the result when both C_{miles} and α are variable using Eq.(7) with the optimal value of $A = 0.9$)

when C_{miles} is assumed to be dependent on wave energy, waves develop more closely to the fetch law, and the excessive wave development seen in the case of constant C_{miles} is improved.

OPTIMIZATION OF DISTRIBUTION RATIO α

In the early stages of wave development, α has to be close to 1, and as the development saturates, α can be expected to approach 0 asymptotically. Therefore, α is formulated as follows.

$$\alpha = -A\overline{\eta^2} + 1 \quad (7)$$

The coefficient A in Eq.(7) is needed to be optimized. The wave growth rate is defined as follows. At each fetch, the significant wave height is calculated from the sea surface height data for 2500 s to 3600 s computation time. The significant wave heights at each fetch are plotted in log-log scale. An approximate line of the significant wave height is obtained. The slope of the approximate line is the wave growth rate. In each wind speed condisiton, the growth rate is calculated by varying A in 0.1 increments from 0.1. The wave growth rate is then compared with the one obtained from the result of the spectral wave model (SWAN; The SWAN team, 2013). The value when the growth rate obtained from XBeach is closest to that of SWAN is taken as the optimal value of A. The wave development and dissipation terms in SWAN are those proposed by Komen et al. (1984).

The optimum values of A were found to be 0.1, 1.6, 0.9, 0.6, and, 0.5 for wind speeds of 10, 20, 30, 40, and 50 m/s, respectively. As an example, the spatial distributions of significant wave height under 30 m/s wind speed conditions are compared (Figure2). The three results are compared: the case when C_{miles} is variable and α is constantly 0.1 (green line), the case when both C_{miles} and α are variable and Eq.(7) for α is introduced using the optimum value of $A = 0.9$ at a wind speed of 30 m/s (cyan line), and the result of SWAN (magenta line). The result when C_{miles} is variable, and $\alpha = 0.1$ (green line) shows that the waves are overdeveloped, particularly in the 100

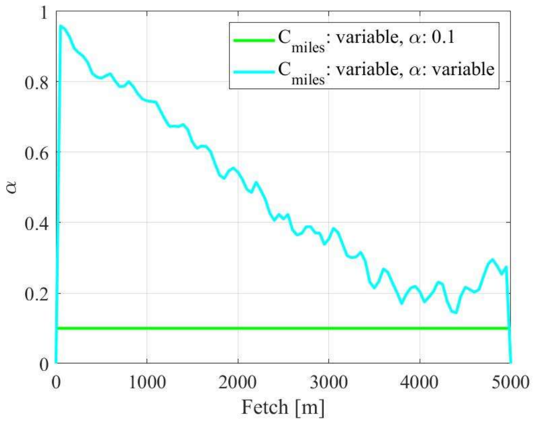

Figure 4 – Spatial distribution of $\boldsymbol{\alpha}$: $\boldsymbol{U}$=30 m/s, 3500 s after the first incident wave input (green: the result when $\boldsymbol{C_{miles}}$ is variable and $\boldsymbol{\alpha}$ is 0.1, cyan: the result when both $\boldsymbol{C_{miles}}$ and $\boldsymbol{\alpha}$ are variable using Eq.(7) with the optimal value of $\boldsymbol{A = 0.9}$)

m to 300 m fetch ranges. On the other hand, in the result that is using variable $\boldsymbol{C_{miles}}$ and $\boldsymbol{\alpha}$ (cyan line), it can be seen that the excessive wave development in that fetch range becomes smaller and that the growth of significant wave heights get closer to the SWAN model result. By introducing Eq.(7) for $\boldsymbol{\alpha}$, wave development that almost follows the fetch law is obtained compared to the case when a fixed value of $\boldsymbol{\alpha}$ is used.

The spatial variation of wave development coefficient $\boldsymbol{C_{miles}}$ and momentum distribution ratio $\boldsymbol{\alpha}$ are computed in the same cases. Figure3 compares the spatial distribution of $\boldsymbol{C_{miles}}$ and Figure4 compares the spatial distribution of $\boldsymbol{\alpha}$ under the 30 m/s wind speed condition. It can be found that both $\boldsymbol{C_{miles}}$ and $\boldsymbol{\alpha}$, which are functions of the variance of the sea surface height, become smaller as the wave development increases with the increase of fetch.

SUMMARY AND DISCUSSION

In this study, a wave development term that includes local wave deformation is introduced into the nonlinear long wave equation with non-hydrostatic pressure, and wind wave development is considered in a phase-resolving wave model. The wave development process is then optimized based on sensitivity experiments. First, a term based on Miles theory is added to the conventional wind stress term. After the introduction, it is found that the wave height increases as the fetch increases, and the wave development is expressed by the added wave development term.

Next, the momentum transport from the wind to the sea surface is divided into a current part and a wave part using the distribution ratio $\boldsymbol{\alpha}$. The equation for $\boldsymbol{\alpha}$ is optimized by comparison with the spectral wave model. As a result, the excessive wave development shown before the introduction of the momentum distribution between currents and waves is improved, and the wave development is found to be close to the fetch law.

In this study, the equation for $\boldsymbol{\alpha}$ is obtained for each wind speed, but considering the practical use of the model, the form of the equation for $\boldsymbol{\alpha}$ that does not depend on wind speed is favorable. In addition, the model obtained in this study does not include the effect of breaking waves. From the above, the general formulation of $\boldsymbol{\alpha}$ independent of wind speed and the introduction of the effect of breaking waves are future issues to be addressed.

REFERENCES

Hirayama Katsuya (2002): Technical note of the port and airport research institute, Port and Airport Research Institute, Japan, 162p. (Japanese)

Honda Tadao, Hisashi Mitsuyasu (1980): Experimental study of wind effect on water surface (Suimen ni oyobosu kaze no sayou ni kansuru jikkentekikenkyu), JSCE, Vol.27, p.90-93. (Japanese)

Miles, John W. (1957): On the generation of surface waves by shear flows, Journal of Fluid Mechanics, Vol.3, pp.185-204.

Mitsuyasu, Hisashi (1985): A note on the momentum transfer from wind to waves, Journal of Geophysical Research: Oceans, Vol. 90, Issue C2, pp.3343-3345.

Mori Nobuhit, Takemi Tetsuya, Kim Sooyoul, Shibutani Yoko, Yasuda Tomohiro, Nakajo Sota, Ninomiya Junichi & Shimura Tomoya (2019): Pesudo prediction experiments of storm surge and waves in 2018 typhoon Jebi by high resolution weather prediction and coupled surge-wave model, JSCE B2(Coastal Engineering), Vol.75, No.2, pp. I_283-I_288. (Japanese)

Pierson, Willard J., Neuman, Gerhard, James, Richard W.(1955): Observing and Fore-casting Ocean Waves by means of Wave Spectra and Statistics, Naval Oceanogr Office, Pub.603, 284p.

Roelvink, Dano, Reniers, Ad, van Dongeren Ap, de Vries, Jaap Vries Thiel, McCall Robert, Lescinski, Jamie (2009): Modelling storm impacts on beaches, dunes and barrier islands, Coastal Engineering, Vol.56, No.11-12, pp.1133-1152.

Shimozono Takenori, Tajima Yoshimitsu, Kumagai Kenzou, Arikawa Taro, Oda Yukinobu, Shigihara Yoshinori, Mori Nobuhito & Suzuki Takayuki (2020): Coastal impacts of super typhoon Hagibis on Greater Tokyo and Shizuoka areas, Coastal Engineering Journal, Vol.62, Issue2, p.129-145.

The SWAN team (2013): SWAN Scientific and technical documentation, SWAN Cycle III version 40.91AB, 113p.